

STRATUS-TOPPED BOUNDARY-LAYER PARAMETERIZATIONS IN LARGE-SCALE MODELS

Chin-Hoh Moeng

NCAR, P.O.Box 3000, Boulder, CO 80307

In this article, I will review and discuss the problems of existing stratus-topped boundary-layer (STBL) parameterizations that have been used in general circulation models (GCMs). I will then describe the current research, using the National Center for Atmospheric Research (NCAR) large-eddy-simulation (LES) code, focused on understanding the STBL and also on evaluating and developing parameterizations. Finally, research needs for the future will be discussed.

1. Problems with Existing Parameterization Schemes

According to the survey reported in *Wyngaard and Moeng* (1989), only three types of STBL parameterizations are used in GCMs: namely, a mixed-layer model used at UCLA and CSU (*Randall et al.* 1985), the Mellor-Yamada Level 2.5 model used at GFDL (*Sirutus and Miyakoda* 1990), and empirical cloud formulae used at BMRC and ECMWF (e.g., *Slingo* 1987). These three types of models will be discussed here.

1.1 Mixed-Layer Modeling

Mixed-layer modeling is a computationally economic way of parameterizing the PBL effect in GCMs since it requires only one vertical layer to represent the whole PBL. This approach assumes that turbulent mixing is highly effective such that all conserved mean fields are well mixed within the PBL. Thus, the details of the dynamics and physics involved can be bypassed. The main closure problem in mixed-layer modeling is to determine the entrainment rate and the cloud amount. So far, the entrainment closures used for the STBL are simply an extension of the entrainment closure for the clear convective PBL, which may not be suitable as discussed later in section 2.1.1.

I list below some major problems in mixed-layer modeling:

- The results are sensitive to the entrainment hypothesis, an unsolved issue for the STBL (e.g., *Randall 1984, Moeng 1987*).
- Assuming that the total moisture mixing ratio is well mixed in the PBL may lead to an over-estimation of the liquid water mixing ratio. Observations and simulations have shown that the total moisture mixing ratio decreases with height within even a highly turbulent PBL. Since the typical liquid water mixing ratio is on the order of 0.5 g/Kg or less (only about 2% of the total mixing ratio), a small over-estimation of the total mixing ratio could lead to a large error in the liquid water estimate.
- Current mixed-layer modeling cannot handle partially cloudy cases. It assumes that air within each GCM grid vertical column is well mixed and therefore is either totally clear or totally cloudy. There is no information of the subgrid-scale variances and covariance of the temperature and moisture fields, which are important in determining the fractional cloud cover.

1.2 Second-Order Closure Modeling

Sirutus and Miyakoda (1990) applied the Mellor and Yamada Level 2.5 model to the GFDL model. The STBL application requires adding the condensation and radiation processes into the traditional turbulent closure modeling. This modeling approach explicitly solves for vertical structure by using multiple grid levels within the PBL; consequently, it needs no entrainment hypothesis. However, the Level 2.5 model is known to poorly represent the third-moment turbulent transport term which is important in redistributing the turbulent kinetic energy in the convective PBL. Accuracy in representing the STBL is therefore questionable.

The major problems in this type of modeling are the following:

- The vertical resolution is still a problem—the current GCM grid resolutions are not fine enough to resolve the marine stratus clouds which are typically less than 300 m in thickness. The main turbulence driving force, i.e., cloud-top radiative cooling, is also poorly resolved.
- There are too many closure assumptions involved in second-order closure modeling. However, the second-order closure modeling results may be less sensitive to these

closure assumptions when compared to the sensitivity of mixed-layer modeling results to entrainment closure. Most of the closures were derived based on laboratory neutral flows that may not be applicable to the STBL.

- The variances and covariance of the temperature and moisture fields cannot be accurately predicted in the Level 2.5 model, thus the model cannot simulate partially cloudy cases.

1.3 Empirical Approach

This approach diagnoses the amount of stratus cloud based on low-level stability and relative humidity (e.g., *Slingo* 1987). Since we now know so little about the STBL processes, the empirical scheme may be a quick fix to the problem of modeling STBL. A major concern is that it is not physically based and may not work for future climate.

2. NCAR LES Research on Marine Stratus Clouds

To develop STBL parameterization schemes, we have first to understand the physical processes involved. At NCAR, the LES method has been used to gain such an understanding. LES has become a very attractive method to treat a turbulent flow field since (1) resolved motions are the energy-containing eddies which are responsible for most the vertical turbulent transport; (2) subgrid scales typically lie within the inertial subrange, thus the subgrid-scale effect can be modeled based on the Kolmogoroff theory; and (3) computing power is increasing rapidly. With current supercomputer power, we are able to use 160 X 160 X 80 grid points on a 2km X 2km X 1km numerical domain; that is, eddies larger than twice the size of the grid mesh—larger than 25m X 25m X 25m—are explicitly resolved. With a typical stratus top at about 500m, the 2km X 2km periodic horizontal domain is enough to cover several large eddies at one instant. Our statistics are computed by averaging not only over the x–y plane but also over a time period of several large-eddy-turnover times. The LES flow fields have been shown to compare well with aircraft observations (e.g., *Shen and Moeng* 1993).

In the following three subsections, I will review some of our recent STBL-LES studies that aim at understanding physical processes, developing a new parameterization for partially cloudy PBLs, and evaluating the system performance of existing parameterizations.

2.1 Studies for Physical Understanding

2.1.1. Surface-Heated vs. Top-Cooled PBLs

Unlike the STBL, existing parameterizations of the clear convective PBL have been shown to be quite adequate. In an attempt to extend the concept of modeling clear-convective PBLs (which mainly are driven by surface heating) to stratus PBLs (which often are driven by cloud-top radiative cooling), *Moeng and Schumann* (1991) examined similarities and differences between the surface-heated and the cloud-top-radiatively-cooled PBLs. In that study, we generated a surface-heated and a top-cooled PBL from LES, retrieved their updraft and downdraft plume structures through conditional sampling, and then compared and analyzed their features. Note that such plumes dominate the features and transport of the PBL turbulence.

In the surface-heated PBL, updraft plumes are initiated and accelerated by the heating-induced buoyancy force, and are active in driving turbulence circulations. Downdrafts are merely the compensating motions of the circulations. Therefore, updrafts are much stronger than downdrafts; they also dominate the transport and entrainment processes.

The cloud-top-cooled PBL looks like an upside down surface-heated PBL, hence one intuitively expects that downdrafts are active and updrafts are passive motions. From our LES analysis, however, we found that, in the top-cooling-driven PBL, downdrafts have about the same strength as updrafts and do not dominate the transport process as do their counterparts, updrafts, in the surface-heated PBL.

To examine this asymmetry, we analyzed the flow fields of these plumes. We found that downdraft plumes are not initiated or pushed down by the cooling-induced buoyancy force; rather, they are initiated by convergence of the horizontal flow branches in turbulent circulations near the cloud top, as illustrated in the sketch (Fig. 1). That particular feature has also been observed in *Nicholls'* (1989) aircraft study. Only after reaching $0.9 z_i$ or farther below the cloud-top level, the downdrafts (that carry most of the cloud-top radiatively-cooled air) found themselves in a warmer environment (that carries little or no radiatively-cooled air), and are then able to drive turbulent circulations. Thus, updrafts and downdrafts drive each other in the following way: In the middle of the PBL, the colder downdrafts drive the turbulent circulations which induce updrafts as the upward branches of the circulations; in the top ~10% of the PBL, however, updrafts are converted to horizontal motions (since they are capped by the inversion layer), and the convergence of these horizontal motions in turn

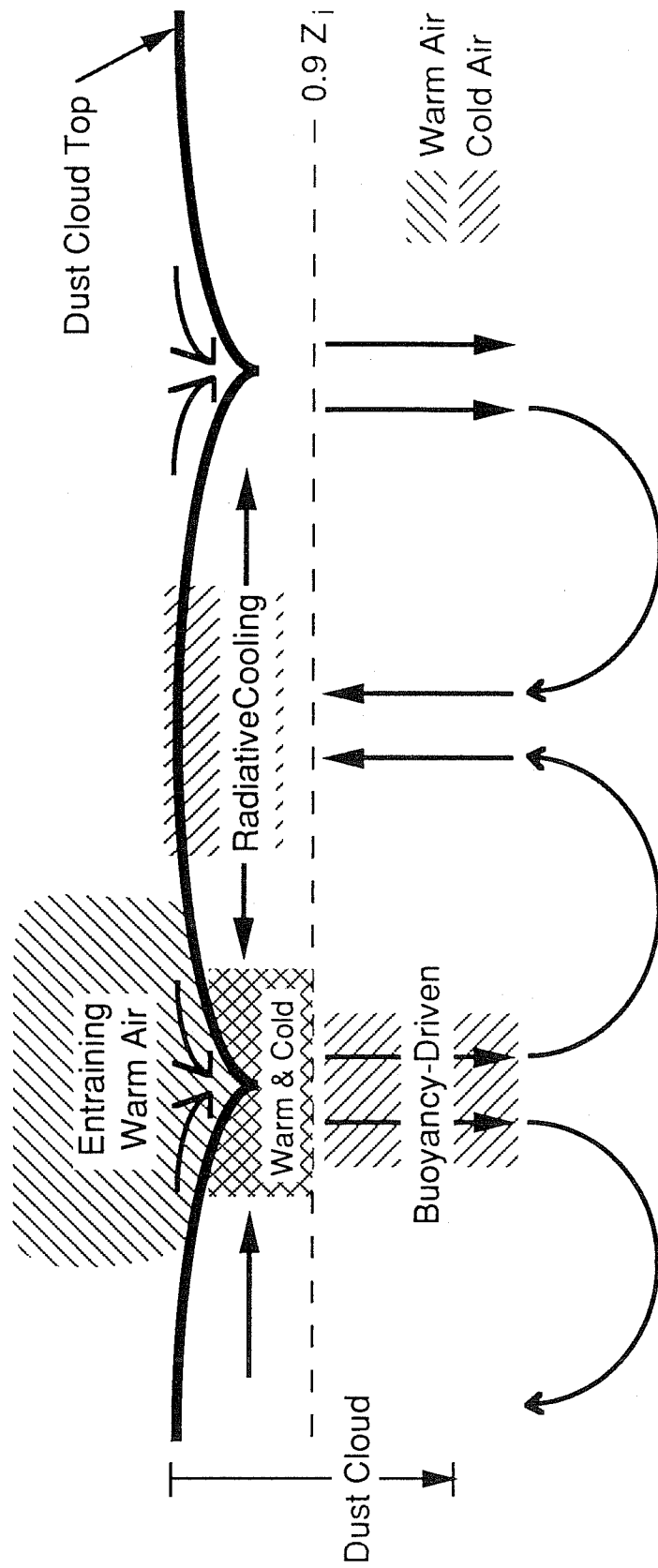


Fig. 1 A sketch of our physical picture showing the idealized flow held (in arrows) and temperature fluctuations (shading) near the top of an idealized cloud-top-coupled PBL. This sketch emphasizes only the locations where the longwave radiative cooling is strongest and where the warm air entrainment is largest.

pushes the air down and forms downdrafts. Thus, it is unlikely that downdrafts can be much stronger than updrafts in the cloud-top-cooled PBL.

This asymmetric role of plumes between the surface-heated and top-cooled PBLs suggests that many of the clear convective PBL modeling concepts cannot be applied to the STBL. For example, the concept of entrainment, and hence its parameterization (for mixed-layer modeling), can be quite different in two cases. In the surface-heated case, entrainment is believed to be driven as strong updrafts impinge on the inversion air and engulf (i.e., entrain) it into the PBL. Consequently, the entrainment buoyancy flux is always about a constant ratio (i.e., -0.2) of the surface buoyancy flux input in the convective clear PBL (with weak shear and a horizontally homogeneous condition). This concept has been used in developing the entrainment hypothesis for mixed-layer modeling (*Ball 1960, Tennekes 1973*).

The entrainment process in the cloud-top-radiatively-cooled PBL, however, is far more complicated. The combined entrained warm air and radiatively cooled air near the cloud top form downdrafts as they are pushed down by convergence of the horizontal motions. If the combined air is cooler than the environment, these downdrafts can eventually drive turbulent circulations. The updraft branches of these circulations then promote entrainment through impingement and engulfment. Therefore, if we have a strong entrainment to begin with, it directly weakens the turbulent circulations because we begin with less cooled air near the cloud top. (Our discussion here excludes the cloud-top entrainment instability condition.) The weaker circulations result in weaker impingement and engulfment, leading to a decrease of the entrainment. This radiation-entrainment self-limiting mechanism has also been pointed out by *Randall et al. (1992)*, based on an equation that was derived by matching the PBL interior mass flux with the entrainment flux at the PBL top. Thus, the entrainment process in the cloud-top-cooled PBL is far more complicated than that in the surface-heated PBL, and one should not expect to simply extend the concept of entrainment hypothesis for the clear convective PBL to that for the STBL. Unfortunately, this clear-convective-PBL entrainment concept is all we have now in deriving the entrainment hypothesis for the STBL.

2.1.2 Roles of Physical Processes to Heat and Moisture Fluxes

The vertical distributions of the heat and moisture fluxes are important in maintaining or dissipating the stratus cloud layer since they determine the warming and moistening of the PBL. Furthermore, the heat and moisture fluxes combined determine the buoyancy flux that

provides the turbulent kinetic energy. Therefore, it is essential to understand the roles of physical processes in determining these fluxes within the STBL.

Moeng et al. (1992) examined the roles of four physical processes: (1) cloud-top longwave radiative cooling (here abbreviated as RAD), (2) entrainment (i.e., ENT), (3) surface heating (i.e., SFC), and (4) evaporative cooling (i.e., EVP). They generated four large-eddy simulations: one corresponds to a dry-cloud-topped PBL with very little surface buoyancy flux, including the first two processes (here denoted as the ENT/RAD case); second, a dry-cloud-topped PBL with a significant amount of surface buoyancy flux, including the first three processes (i.e., ENT/RAD/SFC); third, a wet-cloud-topped PBL with a significant amount of surface heating, including all four processes (i.e., ENT/RAD/SFC/EVP); and fourth, a clear convective PBL, including only the second and third processes (i.e., ENT/SFC). By comparing and analyzing these four simulations using the following procedures, they tried to isolate the role of each process in determining the heat and moisture fluxes.

They first showed that the heat and moisture fluxes can be well expressed as

$$\overline{wc} = 0.6 \sigma_w (C^U - C^D), \quad (1)$$

where c represents a scalar which can be the virtual temperature field, T_v , the liquid moist static energy, h_l or the total moisture mixing ratio, q_T ; σ_w is the root-mean-square of the vertical velocity; and C^U and C^D are the means of the c field within updrafts and downdrafts, respectively. This formula was developed by *Businger and Oncley* (1990) for the clear PBL, and was shown (Figs. 2 and 3) in *Moeng et al.* (1992) to apply very well to the stratus-topped PBL for both temperature and moisture fields. Hence, examining how physical processes contribute to the updraft-downdraft differences ($C^U - C^D$) is almost equivalent to examining how they contribute to the flux, \overline{wc} , with a given turbulent field, σ_w .

In the second step, they conditionally sampled the LES fields to examine the updraft-downdraft differences due to each physical process. Figure 4 shows the mean virtual temperature averaged within all updrafts and all downdrafts, respectively, for all four LES cases. By comparing the first and second cases, we see that the surface heating process increases the $T_v^U - T_v^D$ mostly near the surface and its effect decreases almost linearly with height. Comparing the second and third cases shows that the latent heating effect is small except in the top ~5% in these cases. (The difference near the surface is due to the fact that

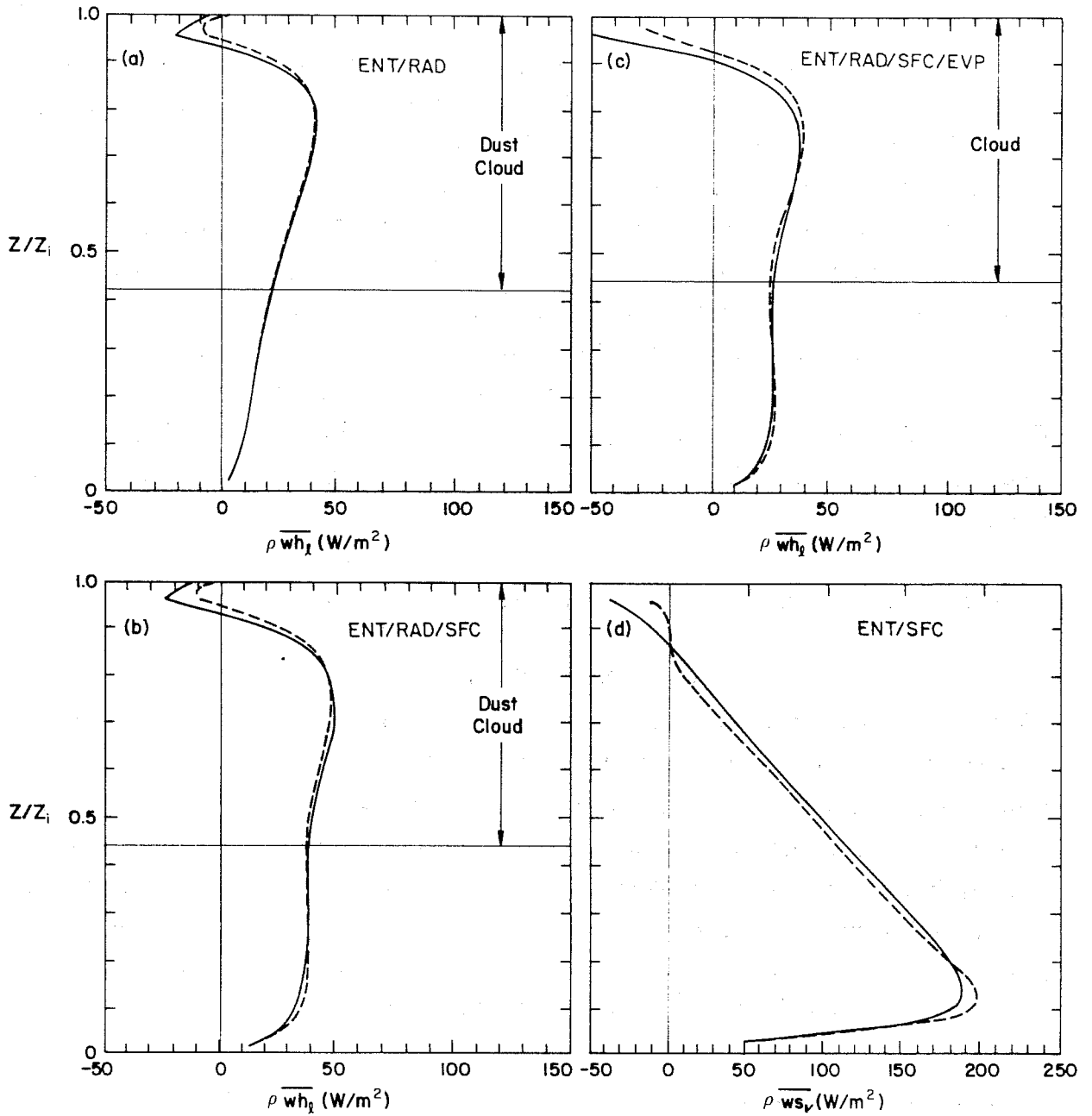


Fig.2 Vertical distributions of $\overline{wh_x}$ (or $\overline{ws_v}$ for the clear case). The solid curves were obtained by correlating the resolved-scale w and h_x (or s_v) of the large-eddy simulated field, and the dashed curves were from Eq. (1), where C^U and C^D were calculated by conditionally sampling the LES field.

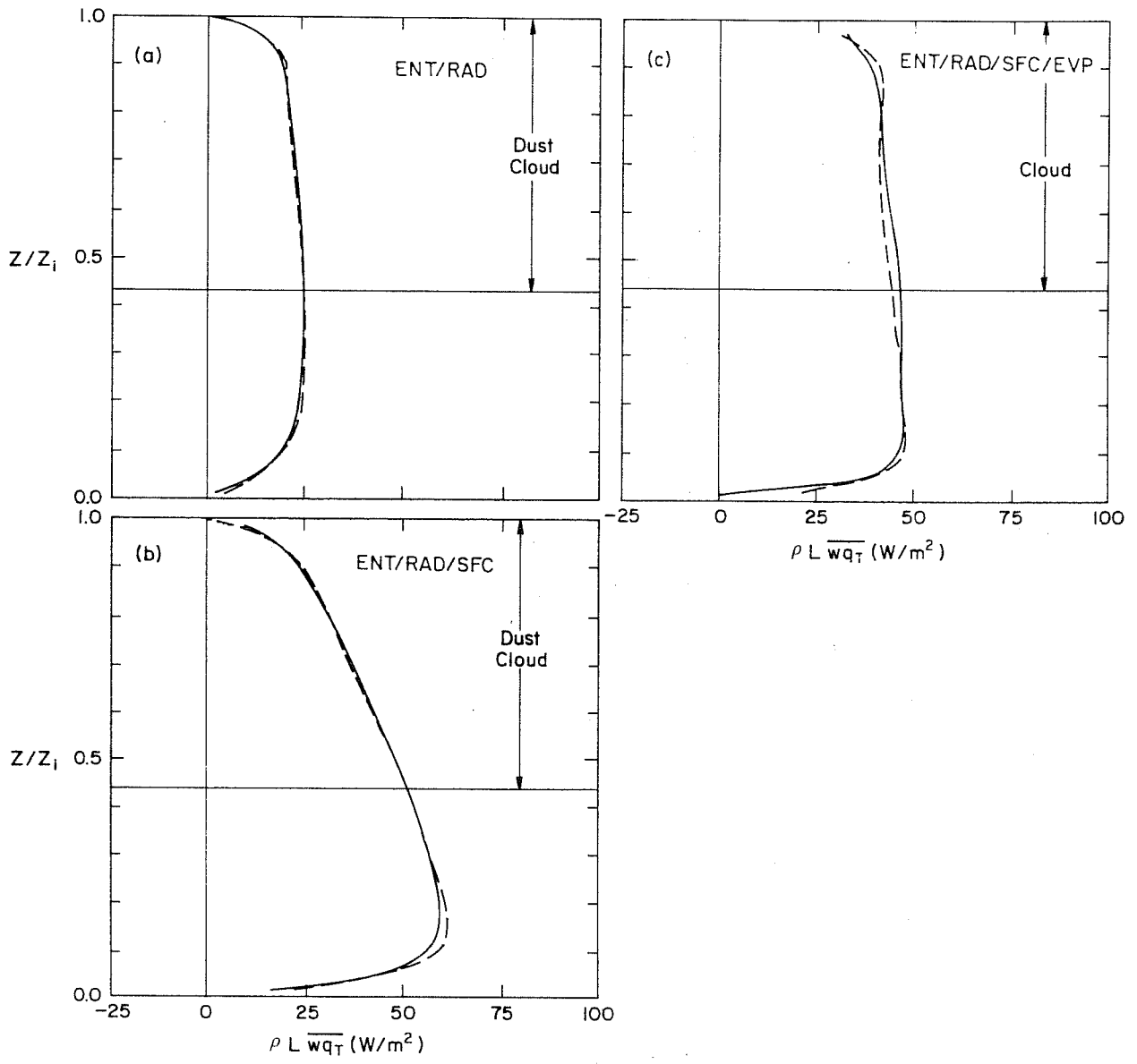


Fig.3 Same as Fig.2 but for $\overline{wq_T}$.

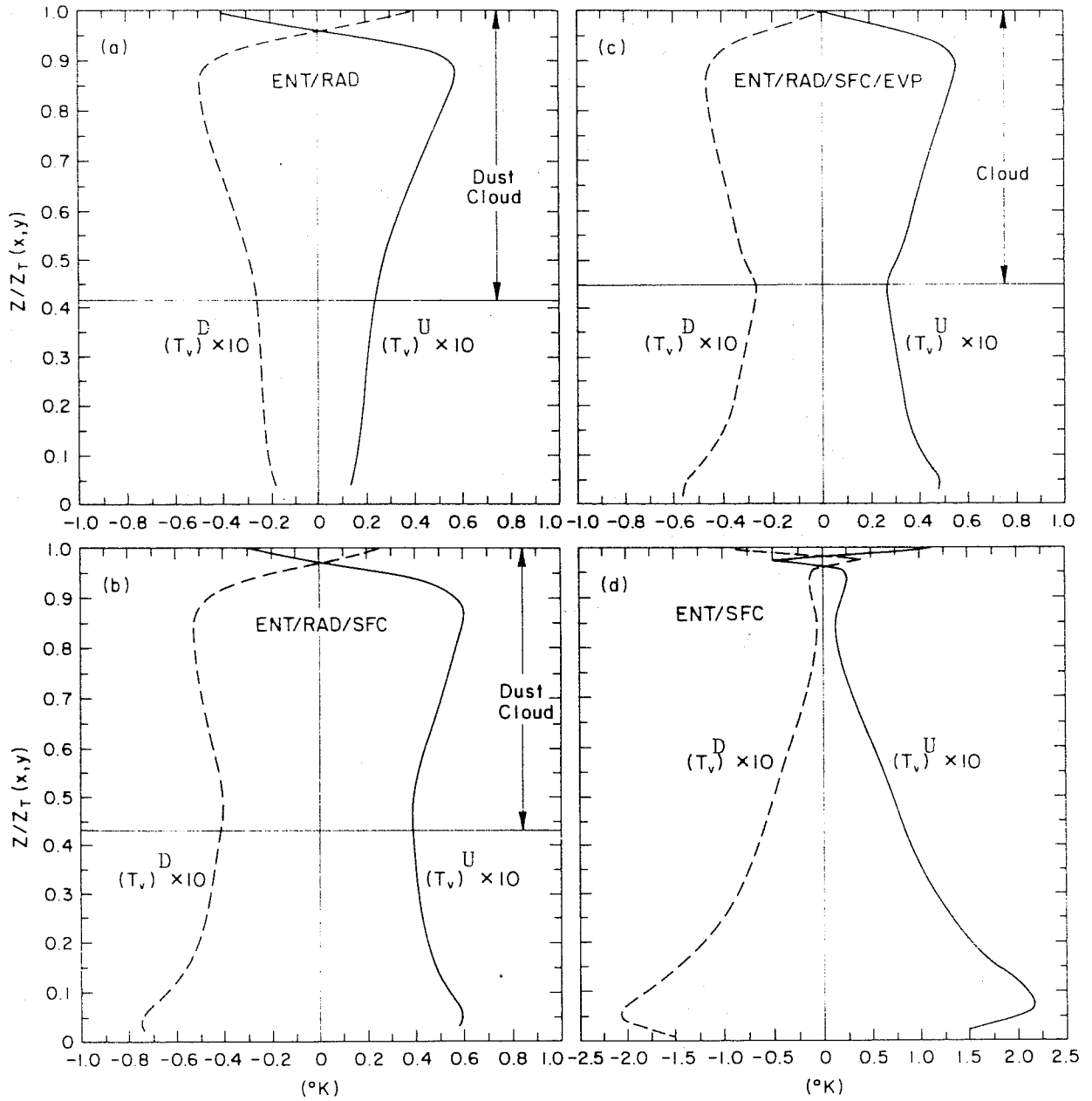


Fig.4 Vertical distributions of the virtual temperature fields averaged within updrafts (solid curves) and within downdrafts (dashed curves). The total horizontal mean value was taken out.

we ran the third case for a longer time period and hence its surface-air temperature and moisture differences are smaller than those in the second case. This results in smaller $T_V^U - T_V^D$ and $q_T^U - q_T^D$ near the surface.)

Comparing the first and fourth cases reveals an interesting feature. The updraft-downdraft temperature difference is less height-dependent in the first case than in the fourth. This can be explained as follows. Cloud-top radiative cooled air is incorporated *mostly into downdrafts*, thus enhancing the $T_V^U - T_V^D$ difference. This effect is largest near the cloud top and decreases downward. On the other hand, entrained warm-inversion air is incorporated also *mostly into downdrafts*, weakening the $T_V^U - T_V^D$ difference. This effect is also largest near the cloud top and decreases downward. In the clear convective PBL, however, the surface heating, *mostly into updrafts*, enhances $T_V^U - T_V^D$, and this effect is maximum near the surface. This enhancement works in an opposite direction from the reduction mechanism due to entrainment. As a result, the $T_V^U - T_V^D$ profile is more height dependent in the fourth case than it is in the first case. This feature suggests to us that all radiative cooling, entrainment, and surface heating contributions to $T_V^U - T_V^D$ take place throughout the *whole* PBL, and are nearly *linear in height*.

Based on this observation and Eq. (1), we may conclude that each contribution of all these three processes (i.e., ENT, RAD, and SFC) to any scalar flux must exist also throughout the whole PBL and are rather linear in height, if the total scalar flux is linear in height. This happens to be the "process partitioning" concept that was proposed by *Manins and Turner* (1978) for the clear PBL case and extended to the stratus-topped PBL by *Stage and Businger* (1981) and *Hanson* (1987). *Moeng et al.* (1992) therefore examined this partitioning approach in the following way. They chose to partition the total heat flux, $H \equiv \overline{wh}_l + F_{rad}$, where \overline{wh}_l is the liquid moist static energy and F_{rad} is the longwave radiation flux, and the total moisture flux $\overline{wq_T}$ since these two fluxes are linear in height in the quasi-steady state. [h_l and T_V are related as $h_l \equiv c_p T_V + gz - Lq_l$, where c_p is the specific heat of air, g gravitational acceleration, z height, L latent heat of condensation, and q_l liquid water mixing ratio.] Note that since F_{rad} is not linear in height, \overline{wh}_l is not linear in height. The H -flux is partitioned into three components: longwave radiative cooling, entrainment, and surface heating. Based on the earlier discussion, all of these three component fluxes can well be linear in height. Figure 5 shows an example, of the ENT/RAD/SFC case, of these three partitioned component fluxes. First, we see that the sum of all three components agrees well

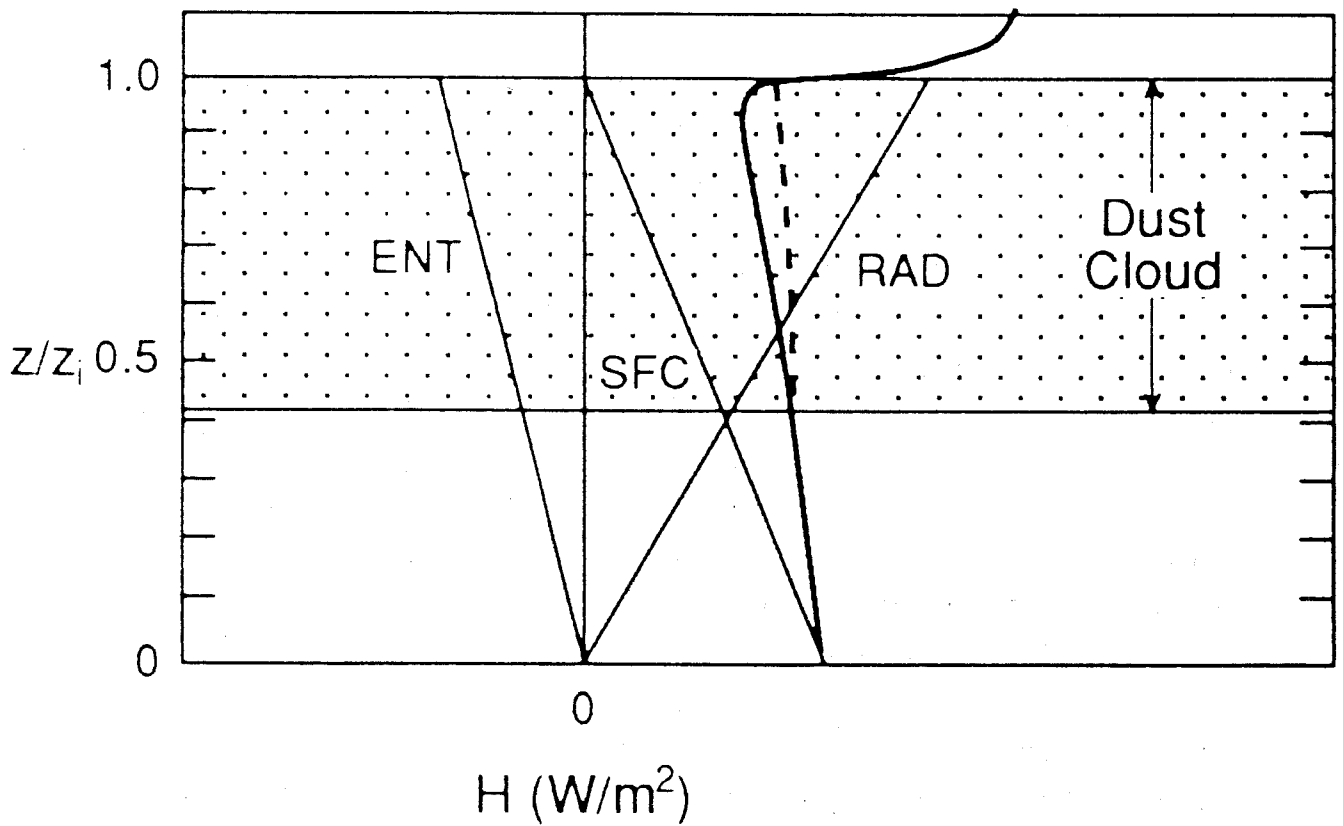


Fig.5 Partitioning of the total thermodynamic energy flux H into the cloud-top radiative cooling process (RAD curve), entrainment (ENT curve), and surface heat flux (SFC curve) for the ENT/RAD/SFC LES case. The sum of all three component fluxes is shown as the dotted curve, and the H -flux computed directly from the LES is shown as the heavy solid curve.

with the H-flux computed directly from the LES case. Second, examining each component contribution to the total flux shows a consistent component contribution comparing to its counterpart contribution to the updraft–downdraft difference given in Fig. 4. For example, the surface heating process contributes to about one-half of the total heat flux at the cloud base level, and that qualitatively agrees with its contribution to $T_V^U - T_V^D$, as shown by comparing Figs. 4a and 4b. The same approach was also applied to the total moisture flux.

This study thus provides a method of (1) *separating the roles* of cloud-top radiative cooling, entrainment, and surface heating effects in determining the net H-flux, and (2) separating the entrainment and surface heating roles in determining the net $\overline{wq_T}$ flux.

2.2 Developing a New Model

By combining the mass flux modeling with the second-order closure approach, *Randall et al.* (1992) developed a new model called the second-order bulk boundary-layer model. This new bulk model has the following three desirable features: (1) it matches the bulk mass fluxes in the interior with the surface and entrainment boundary conditions, (2) it includes a physically based prediction for the fractional area covered by updrafts, and (3) it relaxes the mixed-layer assumption used in earlier bulk models.

Using the mass flux modeling approach, which represents turbulent motions simply by two branches of motions—updrafts and downdrafts—the ensemble average of any scalar, ψ , can be expressed as

$$\overline{\psi} = \psi^U \sigma + \psi^D (1 - \sigma), \quad (2)$$

where ψ^U and ψ^D are the averages of ψ over updraft and downdraft branches, respectively, and σ is the fractional area covered by updrafts. This is a top-hat assumption.

Using Eq. (2), the flux of any species, ψ , in the PBL interior can be written as

$$\overline{w\psi}(z) = M_c(z) [\psi^U(z) - \psi^D(z)], \quad (3)$$

where $\overline{w\psi}$ is the flux of any scalar, ψ , and

$$M_c \equiv \rho \sigma (1 - \sigma) (w^U - w^D), \quad (4)$$

is the convective mass flux. Here w^U and w^D are the mean vertical motions within updrafts and downdrafts, respectively.

In the surface layer, similarity theory gives

$$\overline{w\psi}(\text{at } z_S) = V(\overline{\psi_{S-}} - \overline{\psi_S}), \quad (5)$$

where V , named by Randall the "ventilation mass flux", is the product of surface wind and the drag coefficient that appears in the similarity theory, $S-$ is the earth's surface, and S is the top of the surface layer.

In the entrainment layer, the familiar jump condition gives

$$\overline{w\psi}(\text{at } z_B) = -E(\overline{\psi_{B+}} - \overline{\psi_B}) - \Delta F_R, \quad (6)$$

where E is the entrainment rate, $B+$ and B are the top and the bottom of the entrainment zone, and ΔF_R is the source of ψ (e.g., radiation) within this layer.

Matching (3) with (5) at z_S , and (3) with (6) at z_B , Randall et al. (1992) obtained two "continuity equations" that relate $M_C(z_S)$ to V , and $M_C(z_B)$ to E . By assuming that M_C and σ are independent of height (which is a bulk modeling assumption), Randall et al. obtained

$$M_C = \frac{(E/\chi_E)(V/\chi_V)}{(E/\chi_E) + (V/\chi_V)}, \quad (7)$$

and

$$\sigma = 1 / \left(1 + \frac{E}{V} \frac{\chi_V}{\chi_E} \right), \quad (8)$$

where χ_V and χ_E are the coefficients appearing in the two "continuity equations." Since these two resulting equations do not involve ψ , they must apply for all ψ . Using the LES flow fields, reported in *Schumann and Moeng* (1991) and *Moeng and Schumann* (1991), *Randall et al.* determined the values of χ_V and χ_E , which are 1.22×10^{-2} and 1.02×10^{-2} , respectively.

Once V and E are determined, a common practice in the mixed-layer modeling using the surface similarity theory and an entrainment closure, (7) and (8) can be used to determine M_C and σ .

To relax the well-mixed assumption, Randall et al. used the budget equation of $\overline{\psi^2}$,

$$\frac{\partial}{\partial t} \overline{\psi^2} = -2 \frac{\overline{w\psi}}{\rho} \frac{\partial \overline{\psi}}{\partial z} - \frac{1}{\rho} \frac{\partial}{\partial z} (\overline{\rho w \psi^2}) - 2\varepsilon_\psi, \quad (9)$$

which is zero in a quasi-equilibrium state. The dissipation term, ε_ψ , can be expressed as $\overline{\psi^2}/\tau_{\text{dis}}$, where τ_{dis} is a time scale that characterizes the dissipation rate. Applying the top-hat formula (2) to $\overline{\psi^2}$, and $\overline{w\psi^2}$, the second and third terms in the right-hand-side of (9) become functions of $\overline{w\psi}$, σ , and M_C . By assuming that σ and M_C are independent of height, Eq. (9) becomes a hyperbolic equation that relates $\overline{w\psi}$ and $\partial \overline{\psi} / \partial z$, which is a flux-mean gradient relationship.

This hyperbolic equation can be shown to reduce to two interesting limits: When $\sigma=1/2$, it reduces to a simple downgradient diffusion which is a known property for turbulent transport in a nearly Gaussian flow field. When $\sigma \ll 1$, it reduces to a "compensating subsidence" relationship which is known for a cumulus regime where the vertical velocity field is highly skewed.

Furthermore, by assuming $\partial \overline{\psi} / \partial z$ is constant with height (which may not be appropriate, e.g., see *Moeng and Wyngaard, 1984*), and matching the boundary flux conditions at the top and bottom, Randall et al. showed that this flux--mean gradient equation can be solved analytically for $\overline{w\psi}$ and $\partial \overline{\psi} / \partial z$. A non-zero $\partial \overline{\psi} / \partial z$ thus relaxes the well-mixed assumption.

2.3 Evaluating Existing Models

Another method to develop better PBL parameterization schemes for GCMs is to evaluate the system performance (not individual closure components) of the existing schemes, hoping to form a basis for improvement. For this purpose, a PBL working group was formed at NCAR about three years ago, aiming at developing promising PBL parameterizations for coupled climate models. Our project members include Keith Ayotte, Bill Large, Jim McWilliams,

Chin-Hoh Moeng, Peter Sullivan, and Joe Tribbia (all at NCAR), John Wyngaard (Penn State University), Bert Holtslag (KNMI, the Netherlands), Anders Andren (Uppsala University, Sweden), Pierre Koclas (Canadian Meteorological Center), and Peter Taylor (York University).

Our approach is the following:

- A survey and review of the PBL parameterizations currently used in GCMs and those that have been proposed.
- A classification and coding of the following six generic PBL models:
 - (1) R_i -dependent K (used at, e.g., ECMRW, BMRC),
 - (2) single-point closure (used at GFDL, NMC, GSFC),
 - (3) K-profile (used at OSU, NCAR),
 - (4) mixed-layer (used at UCLA, CSU),
 - (5) multi-stream exchange (including Stull's transilient, Blackadar, and mass-flux models), and
 - (6) stability-bounded models.
- Generation of a database through LESs of different types of PBL.

Our next steps are the following:

- To evaluate the performance of the six models against the LES database and available observations, and
- To develop the most promising PBL parameterizations for the atmosphere-ocean coupled GCM.

Currently, we have generated nine LES databases as shown in Table 1. More realistic LESs (e.g., stably stratified PBL, diurnal and inertial cycles, PBLs over non-uniform and non-smooth surfaces, and in the cumulus regime) and more STBL cases will be generated in the future.

So far, these PBL models are for clear PBLs only; they include no condensation and radiation. To apply this evaluation method to STBL parameterizations, we need first to add condensation and radiation schemes into these models (and also to include new models that are being proposed.) We also need to generate more STBL LES cases. However, we should note here that the LES database has the following limitations: Current simulation flows are limited to a numerical domain of 5 km X 5 km (or less) in horizontal extent. Thus, mesoscale effects on a stratus regime are excluded. Furthermore, because solar radiation and drizzling processes are not yet well understood and not well parameterized, they are currently excluded in the LES. These processes may play important roles in dissipating the stratus cloud regime. We have to rely on observational data for these complicated regimes.

3. Future Research Needs for Developing Parameterizations

Currently, most STBL researchers have focused on studies of cloud maintenance and dissipation, such as cloud-top entrainment instability, cloud decoupling, and the diurnal cycle. However, it is also important to understand the cloud formation.

3.1 Studying Formation of Marine Stratus Cloud

Here, I would like to ask the following questions:

- Do we know well how marine stratus clouds are formed?
- The marine stratus cloud regime often exists over a cold upwelling coastal region. Are they formed as fog or elevated cloud?
- If elevated, there must be turbulent motions that carry the moisture from the ocean surface up to the condensation level. Are these turbulent motions mainly convectively driven where the surface air is even colder than the ocean, i.e., an unstable PBL?
- If the cloud regime is formed in a region where the surface air is warmer than the ocean, i.e., a stable PBL, we have to improve our PBL modeling accordingly, since

Table 1: Large-eddy simulation datasets

Cases	Q^* (K m/s)	U_g (m/s)	Capping Inversion	$\max\{w^*, u^*\}$ (m/s)	z_i (m)	τ_* (s)
1. Convective	0.24	10	Yes	2.0	1030	510
2. Convective/Shear	0.05	15	Yes	0.93	480	516
3. Convective/Shear	0.03	15	Yes	0.79	493	624
4. Shear	0	15	Yes	0.5	448	900
5. Shear (Ekman)	0	15	No	0.4	1440	3600
6. Convective/Shear	0.05	15	No	1.2	1087	890
7. Shear	0	15	No	0.7	1000	2000
8. Stratus-capped	0.02	10	Yes	0.8	510	637
9. Stratus-capped	0	10	Yes	0.8	490	612

(1) mixed-layer models do not work for the stable PBL and (2) most of the second-order closure models underestimate the height of the stable PBL.

We need these answers before starting to develop parameterizations for cloud formation.

3.2 Identifying Datasets for Model Evaluations and Developments

As mentioned, the LES database has several limitations, thus we have to rely on observational data as well. But, are the existing observational datasets, such as the DYCOMS, FIRE, and ASTEX experiments, useful for such STBL model evaluation? The large-scale subsidence motion, W , is a key parameter in determining cloud formation and dissipation. During the ASTEX, the ECMWF model prediction was used to estimate W . In addition, ozone flux measurements were used to estimate the entrainment velocity, thus the W . The question is: How accurate are these W estimates? Furthermore, all existing PBL models consider only turbulent motions. To be useful for evaluating these existing PBL models, we need to filter out the mesoscale effect in observational data. In the future, we certainly need to include both mesoscale and turbulent-scale effects in STBL parameterizations since both play important roles in the stratus-cloud regime. Yet, so far we know so little of how each of these two effects works separately, not to mention their combined effects. My preference is to develop separate schemes for turbulent-scale and mesoscale effects based on our understanding, with the hope that the combination of these separate schemes will work for the combined turbulence-mesoscale effects.

Acknowledgements

I thank Don Lenschow and David Randall for their reviews, and Hope Hamilton for her editing assistance.

REFERENCES

- Ball, F. K., 1960: Control of inversion height by surface heating. *Quart. J. Roy. Meteor. Soc.*, **86**, 483–494.
- Businger, J. A., and S. P. Oncley, 1990: Flux measurement with conditional sampling. *J. Atmos. Oceanic Tech.*, **7**, 349–352.
- Hanson, H. P., 1987: Reinterpretation of cloud-topped mixed-layer entrainment closure. *Tellus*, **39A**, 215–225.

- Manins, P. C. and J. S. Turner, 1978: The relation between flux ratio and energy ratio in convectively mixed layers. *Quart. J. Roy. Meteor. Soc.*, **104**, 39–44.
- Moeng, C.-H., 1987: Large-eddy simulation of a stratus-topped boundary layer. Part II: Implications for mixed-layer modeling. *J. Atmos. Sci.*, **44**, 1605–1614.
- Moeng, C.-H. and U. Schumann, 1991: Composite structure of plumes in stratus-topped boundary layers. *J. Atmos. Sci.*, **48**, 2280–2291.
- Moeng, C.-H., S. Shen, and D. A. Randall, 1992: Physical processes within the nocturnal stratus-topped boundary layer. *J. Atmos. Sci.*, **49**, 2384–2401.
- Moeng, C.-H., and J. C. Wyngaard, 1984: Statistics of conservative scalars in the convective boundary layer. *J. Atmos. Sci.*, **41**, 3161–3169.
- Nicholls, S., 1989: The structure of radiatively driven convection in stratocumulus. *Quart. J. Roy. Meteor. Soc.*, **115**, 487–511.
- Randall, D.A., 1984: Buoyant production and consumption of turbulence kinetic energy in cloud-topped mixed layers. *J. Atmos. Sci.*, **41**, 402–413.
- Randall, D.A., J.A. Abeles, and T.G. Corsetti, 1985: Seasonal simulations of the planetary boundary layer and boundary-layer stratocumulus clouds with a general circulation model. *J. Atmos. Sci.*, **42**, 641–676.
- Randall, D.A., Q. Shao, and C.-H. Moeng, 1992: A second-order bulk boundary layer model. *J. Atmos. Sci.*, **49**, 1903–1923.
- Schumann, U., and C.-H. Moeng, 1991: Plume fluxes in clear and cloudy convective boundary layers. *J. Atmos. Sci.*, **48**, 1746–1757.
- Shen, S., and C.-H. Moeng, 1993: Comparison of a computer-simulated stratus-topped boundary layer with aircraft observations. To appear in *Bound.-Layer Meteor.*
- Sirutus, J., and K. Miyakoda, 1990: Subgrid scale physics in 1-month forecasts. Part I: Experiment with four parameterization packages. *Mon. Wea. Rev.*, **118**, 1043–1064.
- Slingo, J. M., 1987: The development and verification of a cloud prediction scheme for the ECMWF model. *Quart. J. Roy. Meteor. Soc.*, **113**, 899–927.
- Stage, S.A., and J.A. Businger, 1981: A model for entrainment into a cloud-topped marine boundary layer. Part II: Discussion of model behavior and comparison to other models. *J. Atmos. Sci.*, **38**, 2230–2242.
- Tennekes, H., 1973: A model for the dynamics of the inversion above a convective boundary layer. *J. Atmos. Sci.*, **30**, 558–567.
- Wyngaard, J. C., and C.-H. Moeng, 1989: A global survey of PBL models used within GCMs. PBL Model Evaluation Workshop, European Centre for Medium-Range Forecasts, 14–15 August 1989, Reading, UK, eds. P. A. Taylor and J. C. Wyngaard, WCRP Series 42, WMO/TD 378.